



HAL
open science

Random walks with negative particles for discontinuous diffusion and porosity

Hamza Oukili, Rachid Ababou, Gerald Debenest, B. Noetinger

► **To cite this version:**

Hamza Oukili, Rachid Ababou, Gerald Debenest, B. Noetinger. Random walks with negative particles for discontinuous diffusion and porosity. *Journal of Computational Physics*, 2019, 396, pp.687-701. 10.1016/j.jcp.2019.07.006 . hal-02409018

HAL Id: hal-02409018

<https://ifp.hal.science/hal-02409018>

Submitted on 9 Apr 2020

HAL is a multi-disciplinary open access archive for the deposit and dissemination of scientific research documents, whether they are published or not. The documents may come from teaching and research institutions in France or abroad, or from public or private research centers.

L'archive ouverte pluridisciplinaire **HAL**, est destinée au dépôt et à la diffusion de documents scientifiques de niveau recherche, publiés ou non, émanant des établissements d'enseignement et de recherche français ou étrangers, des laboratoires publics ou privés.



Open Archive Toulouse Archive Ouverte

OATAO is an open access repository that collects the work of Toulouse researchers and makes it freely available over the web where possible

This is an author's version published in: <http://oatao.univ-toulouse.fr/25718>

Official URL:

<https://doi.org/10.1016/j.jcp.2019.07.006>

To cite this version:

Oukili, Hamza  and Ababou, Rachid  and Debenest, Gérald  and Noetinger, Benoît *Random walks with negative particles for discontinuous diffusion and porosity*. (2019) *Journal of Computational Physics*, 396. 687-701. ISSN 0021-9991.

Any correspondence concerning this service should be sent to the repository administrator: tech-oatao@listes-diff.inp-toulouse.fr

Random Walks with negative particles for discontinuous diffusion and porosity

H. Oukili ^{a,*}, R. Ababou ^a, G. Debenest ^a, B. Noetinger ^b

^a Institut de Mécanique des Fluides de Toulouse, IMFT, Université de Toulouse, CNRS - Toulouse, France

^b IFP Energies nouvelles, Rueil-Malmaison, France

A B S T R A C T

This study develops a new Lagrangian particle method for modeling flow and transport phenomena in complex porous media with discontinuities. For instance, diffusion processes can be modeled by Lagrangian Random Walk algorithms. However, discontinuities and heterogeneities are difficult to treat, particularly discontinuous diffusion $D(x)$ or porosity $\theta(x)$. In the literature on particle Random Walks, previous methods used to handle this discontinuity problem can be characterized into two main classes as follows: "Interpolation techniques", and "Partial reflection methods". One of the main drawbacks of these methods is the small time step required in order to converge to the expected solution, particularly in the presence of many interfaces. These restrictions on the time step, lead to inefficient algorithms. The Random Walk Particle Tracking (RWPT) algorithm proposed here is, like others in the literature, discrete in time and continuous in space (gridless). We propose a novel approach to partial reflection schemes without restrictions on time step size. The new RWPT algorithm is based on an adaptive "Stop&Go" time-stepping, combined with partial reflection/refraction schemes, and extended with a new concept of negative mass particles. To test the new RWPT scheme, we develop analytical and semi-analytical solutions for diffusion in the presence of multiple interfaces (discontinuous multi-layered medium). The results show that the proposed Stop&Go RWPT scheme (with adaptive negative mass particles) fits extremely well the semi-analytical solutions, even for very high contrasts and in the neighborhood of interfaces. The scheme provides a correct diffusive solution in only a few macro-time steps, with a precision that does not depend on their size.

Keywords:

Diffusion
Random Walk Particle Tracking (RWPT)
Discontinuities
Analytical solutions
Porous materials
Negative particles

1. Introduction

Particle methods have been much used to model the transport of mass, heat, and other quantities through solids, fluids, and fluid-filled porous media. The last two cases involve both diffusive and advective transport phenomena (due to the moving fluid). Hydrodynamic dispersion due to detailed spatial variations of the velocity field has also been modeled as a Fickian diffusion-type process, e.g. in fluid-filled porous structures (see [1]). Other purely diffuse processes include heat diffusion in materials (*Fourier's law*), and pressure diffusion (compressible Darcy flow in a fluid-filled porous medium).

* Corresponding author.

E-mail address: hamza.oukili.01@gmail.com (H. Oukili).

Particle methods are based on a discrete representation of the transported quantity (solute concentration, fluid pressure, fluid saturation, heat or temperature) as discrete packets (the “particles”), each carrying a unit mass, or a unit heat, etc. The advantage of particle methods is that they avoid some of the problems of Eulerian methods based on Partial Differential Equations (PDE’s), such as numerical instability, artificial diffusion, mass balance errors, and/or oscillations that could lead to negative concentrations or saturations. Various types of particle methods have been devised: non-Lagrangian Particle-in-Cell methods (PIC); implementing Markov processes in a PIC framework with stochastic times [2]; continuous-time particles on a grid [3]; the time-domain random walk (TDRW) [4,5]; and Lagrangian particles with discrete time-steps in continuous space (gridless). Such particle methods have been extensively used for modeling advective-diffusive solute transport in porous soils, aquifers, and reservoirs [6].

In “Lagrangian” methods, space is assumed continuous, and particle positions $X(t)$ are real numbers (the method is then “gridless”). In the present work, we focus on Lagrangian particle tracking to solve diffusion processes by random walk (Wiener process), under the generic name RWPT (Random Walk Particle Tracking).

A specific study of the macroscopic behavior of Random Walk particles is necessary when dealing with a heterogeneous or discontinuous diffusion coefficient $D(x)$. The case of discontinuous diffusion is particularly troublesome, and this is our main focus. Such discontinuities occur at “*material interfaces*”, with sudden changes of microstructure (composite materials, layered porous media, *etc.*), and at discontinuities in phase, for example the interface between surface water and groundwater (an important ecological habitat in the hyporheic zone). For solute diffusion in a porous medium, an additional point of interest is the case of discontinuous porosity $\theta(x)$ (if the medium is water-saturated), or discontinuous volumetric water content $\theta(x)$ (if the medium is unsaturated).

In the literature on particle Random Walks, the displacement schemes used for handling the discontinuity can be characterized into two classes: (1) Interface coarsening, interpolation, and drift velocity scheme (e.g. [7,8]); (2) Partial reflection schemes (e.g. [9]). The first class (“interpolation techniques”) smooth out the discontinuity [10]: the interface is coarsened and the parameters (diffusion, porosity) are considered continuous through the coarsened interface. The second class (“partial reflection methods”), introduced by Uffink [9], implements a probabilistic *reflection/transmission* of the particles across the discontinuous interface: probabilities are assigned for particle *reflection* and *transmission* across the interface. Other similar partial reflection/transmission schemes were investigated by [11–17].

Lejay & Pichot [18] proposed a “two-step algorithm” (their Algo.2), equivalent to a Stop&Go procedure: the particle is stopped at the interface, and then undergoes a “Skewed Brownian Motion” (SBM) for the next step, which may lead the particle to cross the interface. Their two-step algorithm was presented for a 1D finite domain with zero flux boundary conditions. On the other hand, they also presented a “one-step algorithm” (their Algo.3) where, it seems, they use a type of acceptance-rejection method to obtain the displacement in the neighborhood of the interface (this method is different from ours). More recently, Lejay & Pichot [19] tested their approaches [18] by implementing 1D benchmark tests, involving comparisons between their SBM and two Random Walks approaches in the literature [9,15].

One of the drawbacks of these approaches is that a small time step is required in order to converge to the correct solution of the discontinuous PDE, even if the number of particles is very large. This is particularly limiting in the presence of many interfaces. This limitation becomes even more drastic for very large diffusion contrasts, e.g., two orders of magnitude or more. Thus, [20,17] showed that the above methods are only valid for infinitesimal time steps. A small time step must be used in order to avoid the overshoot of heterogeneous and discontinuous subregions of space by the particles.

In this study, we propose a novel approach in the framework of “partial reflection methods” but without restrictions on time step size. The new RWPT algorithm is discrete in time and continuous in space (gridless), and the novel aspects have to do with the treatment of discontinuities. The new algorithm is based on adaptive “Stop&Go” time-stepping, combined with partial reflection/transmission schemes similar to [15–18], and extended with the concept of negative mass particles.

This paper is organized as follows. The next section, 2, presents the theory behind Random Walk Particle Tracking methods (RWPT), and the corresponding macroscopic diffusion PDE. Section 3 presents a novel particle-based method for solving heterogeneous and discontinuous transport problems using RWPT with “negative mass particles”. Section 4 compares analytical solutions to our RWPT results. Section 5 recapitulates the method and discusses extensions of this work.

2. Theory

This section presents the theory of advective-diffusive transport, namely, the concentration-based, macroscopic PDE’s, and the related theory of Stochastic Differential Equations (SDE’s) driven by white noise, governing particles at the microscopic scale.

2.1. Concentration based PDE’s

2.1.1. The Gaussian function (PDF)

Let us define a Gaussian PDF, denoted $G(\mu, \sigma^2, x)$, where μ is the mean, σ^2 the variance, and $x = X(t)$ the particle position at any fixed time t :

$$\forall x \in \mathbb{R}; \quad G(\mu, \sigma^2, x) = \frac{1}{\sigma \sqrt{2\pi}} \exp\left(-\frac{(x - \mu)^2}{2\sigma^2}\right) \quad (2.1)$$

A Gaussian random variable (RV) with mean μ and variance σ^2 is denoted $N(\mu, \sigma^2)$ and has the Probability Density Function (PDF) $G(\mu, \sigma^2, x)$. Letting $\sigma^2 = 2D_0t$, this Gaussian PDF represents the macroscopic concentration solution $C(x, t)$ of the diffusion PDE with spatially constant diffusion coefficient D_0 , for an initial point source condition $C(x, t) = M_0\delta(x - \mu)$, with unit mass $M_0 = 1$, in an infinite domain.

2.1.2. The advection-diffusion transport PDE for concentration

The equation governing the transport of solute concentration (C) in a heterogeneous medium with variable parameters \mathbf{D} (diffusion coefficient), θ (porosity) and \mathbf{V} (velocity) is (see for instance [11]):

$$\begin{aligned} \frac{\partial(\theta C)}{\partial t} &= \nabla \cdot (-\theta \mathbf{C}\mathbf{V} + \mathbf{D} \cdot \nabla(\theta C)) \\ &= -\nabla \cdot \{\theta C (\mathbf{V} + \nabla \cdot \mathbf{D} + \mathbf{D} \cdot \nabla(\ln \theta))\} + \frac{1}{2} \nabla \cdot \nabla \cdot (2\theta \mathbf{C}\mathbf{D}) \end{aligned} \quad (2.2)$$

Note that we do not distinguish between vectors and second rank tensors. The first equality corresponds to the conservative (divergence) form of the PDE, while the second equality corresponds to its decomposed form (from which apparent “drift velocity” terms emerge due to spatially variable diffusion and porosity coefficients).

For a 1D problem with scalar diffusion D , the transport PDE for an initial source at $x = x_0$ in a homogeneous medium with constant parameters D , θ and V is:

$$\begin{cases} \forall t > 0; \forall x \in \mathbb{R}; & \frac{\partial C}{\partial t}(x, t) = -V \frac{\partial C}{\partial x}(x, t) + D \frac{\partial^2 C}{\partial x^2}(x, t) \\ \forall t > 0; & \lim_{x \rightarrow \pm\infty} C(x, t) = 0 \\ \forall x \in \mathbb{R}; & C(x, 0) = \frac{M_0}{\theta} \delta(x - x_0) \end{cases} \quad (2.3)$$

The last equation represents an initial point source located at $x = x_0$ with mass M_0 , and $\delta(x)$ represents the Dirac pseudo-function (δ distribution) (e.g. Schwartz [21]).

This PDE will be later formulated for purely diffusive discontinuous diffusion and porosity coefficients in section 2.2.

The analytical solution of Eq. (2.3) is:

$$\forall t > 0; \forall x \in \mathbb{R}; \quad C(x, t) = \frac{M_0}{\theta} G(x_0 + Vt, 2Dt, x) \quad (2.4)$$

where G is the Gaussian PDF defined in Eq. (2.1).

2.1.3. From concentration to particle positions

Let us consider now a particle based method to solve Eq. (2.3). The concentration can be expressed as follows [22,23]:

$$C(x, t) = \int_{\mathbb{R}} C(X_t, t) \delta(X_t - x) dX_t = \int_{\mathbb{R}} \delta(X_t - x) dm_t \quad (2.5)$$

where X_t and dm_t represent, respectively, the position and mass of an infinitesimal concentration packet (to be discretized as a “particle”).

The PDF of particles positions at any fixed time t should follow the distribution $G(x_0 + Vt, 2Dt, x)$. Thus, the corresponding particle positions can be generated using a Gaussian RV:

$$X_t = N(x_0 + Vt, 2Dt) = x_0 + Vt + \sqrt{2Dt} N(0, 1) \quad (2.6)$$

where $N(0, 1)$ designates a normalized Gaussian RV (zero mean and unit variance). For $V = 0$, (X_t) is the Wiener process. As can be seen, the PDF of (X_t) is identical to the concentration solution in Eq. (2.4) divided by M_0 .

In the case of spatially variable but differentiable coefficients $D(x)$ and $\theta(x)$, the corresponding SDE becomes [22,11,24]:

$$X_{t+dt} = X_t + \sqrt{2D(X_t)dt} N(0, 1) + \{V(X_t) + \nabla(D(X_t)) + D(X_t) \nabla(\ln \theta(X_t))\} dt \quad (2.7)$$

which governs the Gaussian Markovian process (X_t) . After “explicit” “discretization”, dt is replaced with the finite Δt step [7–9,12,25,13–17].

However, if $D(x)$ or $\theta(x)$ is discontinuous, the SDE Eq. (2.7) does not hold.

2.2. Prototype problem: 1D diffusion with a single source and a single discontinuity

In this section, we define a purely diffusive problem, with an initial Dirac source, in an infinite porous medium comprising two subdomains Ω_1 and Ω_2 separated by a single discontinuity, or “material interface”. The interface is located at $x_{1-2} = 0$, and the initial point source is located at $X_{Source} = x_0 < 0$. The subdomains Ω_1 and Ω_2 have different diffusion coefficients D_1 and D_2 , and different porosities θ_1 and θ_2 . Such discontinuities can be found in soils, fractured rocks, and many other porous materials. For instance, [8] studied oxygen diffusion through a discontinuous grains/joints system in a submicron layer of Nickel Oxide.

Here, to illustrate our RWPT method (as in Labolle’s analysis [11]), we focus on 1D solute diffusion in a porous medium with a single interface, where both $D(x)$ and $\theta(x)$ are discontinuous. The PDE system for the discontinuous problem is, for the domain $\Omega = \Omega_1 \cup \Omega_2$:

$$\forall t > 0; \forall x \in \Omega_i; \quad \frac{\partial (\theta_i C_i)}{\partial t} = \frac{\partial}{\partial x} \left(\theta_i D_i \frac{\partial C_i}{\partial x} \right) \quad (2.8a)$$

$$\forall t \geq 0; \quad \lim_{x \rightarrow \pm\infty} C_i(x, t) = 0 \quad (2.8b)$$

$$\begin{cases} \forall t \geq 0; & C_1(x_{1-2}, t) = C_2(x_{1-2}, t) \\ \forall t \geq 0; & -\theta_1 D_1 \frac{\partial C_1}{\partial x}(x_{1-2}, t) = -\theta_2 D_2 \frac{\partial C_2}{\partial x}(x_{1-2}, t) \end{cases} \quad (2.8c)$$

$$\forall x \in \Omega_i; \quad C_i(x, 0) = \frac{M_0}{\theta_i} \delta(x - x_0) \quad (2.8d)$$

In Eq. (2.8a), each PDE represents a mass conservation equation for the solute in each subdomain. In the case at hand, porosities θ_1 and θ_2 are constant in each subdomain and can be factored out from each PDE. The system (2.8c) enforces the continuity of solute concentration (mass per volume of solvent) and of areal solute flux density. In all these equations, Fick’s law is used for the diffusive flux.

The analytical solution of problem 2.8 is given by C_1 and C_2 ($\forall t \geq 0$):

$$(\Omega_1) : \forall x \leq x_{1-2}; \quad C_1(x, t) = C_1^S(x, t) + C_1^R(x, t) \quad (2.9a)$$

$$C_1^S(x, t) = \frac{M_0}{\theta_1} G(x_{1-2} + (x_0 - x_{1-2}), 2D_1 t, x) \quad (2.9b)$$

$$C_1^R(x, t) = \frac{M_0}{\theta_1} R_{1-2} G(x_{1-2} - (x_0 - x_{1-2}), 2D_1 t, x) \quad (2.9c)$$

$$(\Omega_2) : \forall x \geq x_{1-2}; \quad C_2(x, t) = \frac{M_0}{\theta_2} (1 - R_{1-2}) \times G(x_{1-2} + \beta_{1-2}(x_0 - x_{1-2}), 2D_2 t, x) \quad (2.9d)$$

$$R_{1-2} = \frac{\theta_1 \sqrt{D_1} - \theta_2 \sqrt{D_2}}{\theta_1 \sqrt{D_1} + \theta_2 \sqrt{D_2}} \quad \text{and} \quad \beta_{1-2} = \frac{\sqrt{D_2}}{\sqrt{D_1}} \quad (2.9e)$$

- C_1^S (“S” for “Source”) is the solution of this diffusion problem without interface (no discontinuities).
- C_1^R is the symmetric of C_1^S relative to the interface $x = x_{1-2}$, multiplied by coefficient R_{1-2} (R for Reflection).
- C_2 is the solution of a diffusion problem with initial mass $M_0(1 - R_{1-2})$ located at $x_{1-2} + \beta_{1-2}(x_0 - x_{1-2})$.

Eqs. (2.9) extend previous analytical solutions given by [26,7,27].

3. Methods and algorithms

In this section, we start by explaining the need for a new algorithm to deal with discontinuities. Then we discuss previous methods proposed in the literature. Finally, we present our new method and discuss its advantages compared to the previous ones.

3.1. Discontinuity problem for Random Walk

The most straightforward test of an algorithm for diffusion with discontinuous $D(x)$ is the “uniform concentration test”, where the exact solution of the diffusion PDE is constant concentration $C(x, t) = C_0$ at all times (t) and all positions (x). This is obtained by imposing constant initial concentration $C(x, 0) = C_0$, and imposing either zero flux conditions $\partial C / \partial x = 0$, or else Dirichlet conditions $C = C_0$, at both boundaries.

The random walk equation can be written as follows for 1D diffusion with variable $D(x)$:

$$X^{(p)}(t_n + \Delta t_n) = X^{(p)}(t_n) + \Delta t_n \frac{\partial D}{\partial x} \left(X^{(p)}(t_n) \right) + \sqrt{2D(X^{(p)}(t_n)) \Delta t_n} Z^{(p)}(t_n) \quad (3.1)$$

However, this equation is limited to the case of continuously variable diffusion coefficient. Let us now focus on the case of discontinuous $D(x)$. If we naïvely insert the discontinuous $D(x)$ in the above equation, a deficit of concentration appears near the interface of discontinuity, where $D_1 < D_2$. We can deal with this deficit of concentration using two different schemes (reflection, smoothing). For this purpose, a Stop&Go algorithm is necessary; it is described in the following section.

3.2. Partial reflection and extensions (algorithm)

3.2.1. Partial reflection scheme for the case $R_{1-2} \geq 0$

The general principle of this partial reflection scheme, so far, is similar to the one previously used in literature [15–17]. The fractions $|R_{1-2}|$ and $(1 - |R_{1-2}|)$ are interpreted as probabilities. The issue of “negative probabilities” will be tackled later below and in section 3.2.2. Here, we focus on $R_{1-2} \geq 0$.

Thus, the displacement algorithm for $X(t)$ becomes:

$$\begin{cases} \llbracket R_{1-2} \rrbracket = 1; & X(t) = x_{1-2} - N(x_0 - x_{1-2}, 2D_1 t) : \{X^{Rl} \text{ reflected}\} \\ \llbracket R_{1-2} \rrbracket = 0; & X(t) = x_{1-2} + \sqrt{\frac{D_2}{D_1}} N(x_0 - x_{1-2}, 2D_1 t) : \{X^{Rr} \text{ refracted}\} \end{cases} \quad (3.2)$$

where $\llbracket R_{1-2} \rrbracket$ designates a Bernoulli RV that is equal to 1 with probability $|R_{1-2}|$ and equal to 0 with probability $(1 - |R_{1-2}|)$, x_0 is the initial particle position $X(0)$, and x_{1-2} is the interface position.

However, until now we have considered only the absolute value of R_{1-2} . Thus, the previous algorithm is sufficient *only* in cases where R_{1-2} is positive.

3.2.2. Partial reflection scheme for the case $R_{1-2} < 0$

Negative partial reflection probability R_{1-2} corresponds to a subtraction in the analytical solution ($C(x, t)$). However, it is difficult to “subtract” particles at a specific location (position) with RWPT compared to adding particles. The reason is that, when attempting to subtract a particle at a specified location, one has to act indirectly by searching for particles in a neighborhood of the desired location, while adding a particle at a specific location is always possible directly. This subsection discusses a new method to deal with negative R_{1-2} for a single interface (we have also extended the method to multiple interfaces in the next subsection).

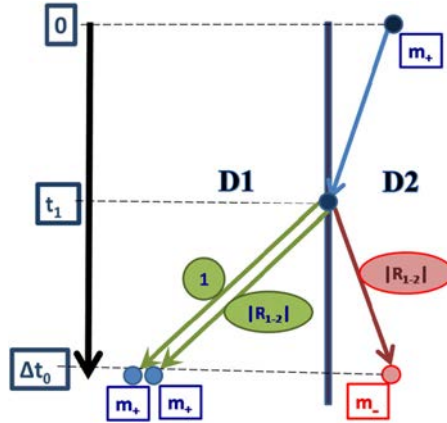


Fig. 3.1. Partial reflection scheme with negative mass particles, for a domain with discontinuous diffusion and porosity (e.g., here, $D_2 < D_1$). Each given particle arriving at the interface with negative R_{1-2} is transmitted with probability 1. In addition, two particles with opposite masses pop up with $|R_{1-2}|$ probability.

For the case of negative R , we propose the following algorithm. First, the particle is always refracted. Secondly, with probability $|R_{1-2}|$, two new particles are created: one is refracted and has the same mass as the original particle, and the other is reflected with a mass of opposite sign (Fig. 3.1). This algorithm allows us to model the exact solution to the discontinuous diffusion problem. Thus, the displacement algorithm for each particle $X_k(t)$ becomes:

$$\begin{cases} X_k(t) = x_{1-2} + \sqrt{\frac{D_2}{D_1}} N(x_0 - x_{1-2}, 2D_1 t) \{ \text{refracted} \} \\ \llbracket R_{1-2} \rrbracket = 1; & X_k^{pos}(t) = x_{1-2} + \sqrt{\frac{D_2}{D_1}} N(x_0 - x_{1-2}, 2D_1 t) \{ \text{refracted} \} \\ \llbracket R_{1-2} \rrbracket = 1; & X_k^{neg}(t) = x_{1-2} - N(x_0 - x_{1-2}, 2D_1 t) \{ \text{reflected} \} \end{cases} \quad (3.3)$$

with the particle X_k^{pos} has the same mass as X_k and the particle X_k^{neg} has the mass of X_k multiplied by (-1) .

3.3. Multiple interfaces

After crossing one interface, a particle could eventually cross a second interface. The algorithm should be able to deal with any number of interfaces crossed by a given particle, in a single time step.

3.3.1. Semi-analytical solution for a diffusion problem with $N \geq 2$ interfaces

To obtain the RWPT algorithm that deals with multiple interfaces, let us first generalize the solution Eq. (2.9) of Eq. (2.8) for N -interfaces and $(N + 1)$ layers. The generalization of Eq. (2.8) for $i \in \llbracket 1; N + 1 \rrbracket$ is:

$$\forall t > 0; \forall x \in \Omega_i; \quad \frac{\partial (\theta_i C_i)}{\partial t} = \frac{\partial}{\partial x} \left(\theta_i D_i \frac{\partial C_i}{\partial x} \right) \quad (3.4a)$$

$$\begin{cases} \forall t \geq 0; & \lim_{x \rightarrow -\infty} C_1(x, t) = 0 \\ \forall t \geq 0; & \lim_{x \rightarrow +\infty} C_{N+1}(x, t) = 0 \end{cases} \quad (3.4b)$$

$$\begin{cases} \forall t \geq 0; \forall i \in \llbracket 1; N \rrbracket & C_i(x_{i,i+1}, t) = C_{i+1}(x_{i,i+1}, t) \\ \forall t \geq 0; \forall i \in \llbracket 1; N \rrbracket & -\theta_i D_i \frac{\partial C_i}{\partial x}(x_{i,i+1}, t) = -\theta_{i+1} D_{i+1} \frac{\partial C_{i+1}}{\partial x}(x_{i,i+1}, t) \end{cases} \quad (3.4c)$$

$$\forall x \in \Omega_i; \quad C_i(x, 0) = \frac{M_0}{\theta_i} \delta(x - x_0) \quad (3.4d)$$

The solution Eq. (2.9) is composed of three gaussians, one of which ($C_1^S(x, t)$) is the solution of a pure diffusive problem, and the other two depend on C_1^S and on the interface position. Let us define two linear operators L_{ij} and L_{ij}^* :

$$L_{ij}(G(x_0, 2D_i t, x)) = R_{ij} G(2x_{i-j} - x_0, 2D_i t, x) \quad (3.5)$$

$$L_{ij}^*(G(x_0, 2D_i t, x)) = (1 - R_{ij}) G\left(x_{ij} + \sqrt{\frac{D_j}{D_i}}(x_0 - x_{i-j}), 2D_j t, x\right) \quad (3.6)$$

Thus the solution Eq. (2.9) could be written as follows:

$$\begin{cases} \forall t > 0; \forall x \leq x_{1-2}; & C_1(x, t) = C_1^S(x, t) + L_{12}(C_1^S(x, t)) \\ \forall t > 0; \forall x \geq x_{1-2}; & C_2(x, t) = L_{12}^*(C_1^S(x, t)) \end{cases} \quad (3.7)$$

The decomposition (Eq. (3.7)) can be further generalized: for each individual interface, new gaussians are generated, with parameters chosen to fit the solution. Hence, each time a gaussian function g initially in a subdomain (i) encounters an interface at position x_{i-j} , we add $L_{i,j}(g)$ to the solution in subdomain (i) and $L_{i,j}^*(g)$ to the solution in subdomain (j). See Algorithm 1.

Algorithm 1 Semi-analytical solution for diffusion with $N \geq 2$ interfaces.

1. C_k concentration in subdomain k
 2. Initialize $C_i k = C_S$ with C_S the solution of a diffusion problem with no discontinuity.
 3. $u_k = \pm 1$ the direction towards the interfaces limiting subdomain (k).
 4. **while** (C_k) not converged **do**
 - (a) $C_k = C_k + L_{k,k+u_k}(C_i k)$ and $C_{k+u_k} = C_{k+u_k} + L_{k,k+u_k}^*(C_i k)$
 - (b) $u_{k+u_k} = u_k$ and $u_k = -u_k$
 - (c) $C_i k = L_{k,k+u_k}(C_i k)$ and $C_{k+u_k} = C_{k+u_k} + L_{k,k+u_k}^*(C_i k)$
 5. **end**
-

For the two-interface problem ($N = 2$), the previous algorithm leads to an analytical solution for diffusion with an initial source, with discontinuous diffusion coefficients and porosities having three different values (three layers). Thus the analytical solution for a source located at the position x_0 in subdomain ($i = 1$), $\forall t \geq 0$:

$$\begin{cases} \forall x \leq x_{1;2}; & \frac{\theta_1}{M_0} C_1(x, t) = id + L_{12} + \sum_{i=0}^{+\infty} L_{21}^* (L_{23} L_{21})^i L_{23} L_{12}^* \\ \forall x_{1;2} \leq x \leq x_{2;3}; & \frac{\theta_2}{M_0} C_2(x, t) = \sum_{i=0}^{+\infty} (id + L_{23}) (L_{21} L_{23})^i L_{12}^* \\ \forall x \geq x_{2;3}; & \frac{\theta_3}{M_0} C_3(x, t) = L_{23}^* \sum_{i=0}^{+\infty} (L_{21} L_{23})^i L_{12}^* \end{cases} \quad (3.8)$$

with the right side of Eq. (3.8) is applied to $G(x_0, 2D_1 t, x)$.

The analytical solution for a source located at the position x_0 in subdomain ($i = 2$), $\forall t \geq 0$:

$$\left\{ \begin{array}{l} \forall x \leq x_{1;2}; \quad \frac{\theta_1}{M_0} C_1(x, t) = L_{21}^* \sum_{i=0}^{+\infty} (L_{23} L_{21})^i (id + L_{23}) \\ \forall x_{1;2} \leq x \leq x_{2;3}; \quad \frac{\theta_2}{M_0} C_2(x, t) = \sum_{i=0}^{+\infty} (id + L_{21}) (L_{23} L_{21})^i (id + L_{23}) \\ \forall x \geq x_{2;3}; \quad \frac{\theta_3}{M_0} C_3(x, t) = L_{23}^* \sum_{i=0}^{+\infty} (L_{21} L_{23})^i (id + L_{21}) \end{array} \right. \quad (3.9)$$

with the right side of Eq. (3.8) is applied to $G(x_0, 2D_2t, x)$.

This solution is detailed in Appendix A, and it has been verified by substitution into the governing PDE's.

3.3.2. Generalization of the RWPT algorithm for $N \geq 2$ interfaces

The same idea of generalization of the analytical solution in subsection 3.3.1 (from one interface into a multi-interface) has been applied to the RWPT method for a problem with N interfaces. If a particle crosses an interface, then (step 1) its position is altered according to previous algorithms that deal with discontinuities (see subsection 3.2, Eq. (3.2) for $R \geq 0$ and Eq. (3.3) for $R < 0$). After this (step 2), if the new particle position does not belong to its initial subdomain, nor to the adjacent subdomains, then go back to "step 1". Thereafter, the particle continues undergoing this algorithm within a conditional loop, until the particle does not cross an interface (it then reaches its final position within the loop). See Algorithm 2.

Algorithm 2 RWPT algorithm for $N \geq 2$ interfaces.

1. Consider particle (k) with mass m_k and position X_k .
 2. **while** particle (k) crosses interfaces **do**
 - (a) **if** $R_{1,2} \geq 0$ **then**
 - i. **if** $\llbracket R_{1,2} \rrbracket = 0$; **then** the particle (k) is *refracted* to the position X_k^{Rr} as in Eq. (3.2) **endif**
 - ii. **if** $\llbracket R_{1,2} \rrbracket = 1$; **then** the particle (k) is *refracted* to the position X_k^{Rl} as in Eq. (3.2) **endif**
 - (b) **Else** (case $R_{1,2} < 0$)
 - i. The particle (k) is *refracted* to the position X_k^{Rr} .
 - ii. **if** $\llbracket R_{1,2} \rrbracket = 1$; **then** Create two particles "A" and "B":
 - A. with mass m_k and at the *refracted* position X_k^{Rr} .
 - B. with mass $-m_k$ and at the *refracted* position X_k^{Rl} .
 - iii. **endif**
 - (c) **end**
 3. **end**
-

This algorithm will be tested in section 4, with the analytical solution defined in subsection 2.2. Then, it will be compared with a generalized analytical solution for a pure diffusion problem with two interfaces and three different diffusion coefficients and water contents: the detailed analytical solution for this 3-layer case is presented in Eq. (3.8). And finally, it will be validated with an even more generalized semi-analytical solution which algorithm has been detailed in the previous subsection 3.3.1.

3.4. Post processing: from particles to concentrations

Post-processing in Random Walk method is essential since the primary objective of the simulation is to get the concentration (temperature or pressure) field. A special attention should be given to Negative unit mass and Adaptive mass particle methods in particular, since they are very different from the classical Random Walk simulation. Here, mass conservation is still maintained, since each time we create a negative mass, we create also a positive one.

The macroscopic concentration is determined from the distribution of particle positions X_t weighted by their respective masses, $dm_t = C(X_t, t) dX_t$. This can be expressed formally as¹:

$$C(x, t) = \int_{\mathbb{R}} C(X_t, t) \delta(X_t - x) dX_t = \int_{\mathbb{R}} \delta(X_t - x) dm_t \quad (3.10)$$

¹ More precisely, in a given domain Ω , the local concentration $C(\mathbf{x}, t)$ is related to the PDF of particle positions $f_{X_t}(\mathbf{x}; t)$ by $C(\mathbf{x}, t) = M_{\Omega}(t) f_{X_t}(\mathbf{x}; t)$ where $M_{\Omega}(t)$ is the total mass of the particles inside the domain Ω at time t .

The most basic one is the Fixed Windows method, which we use here (section 4). The domain is meshed, and the concentration is simply calculated on discrete node-centered cells by summing the masses of the particles in each cell and dividing by the volume of the cell. It is basically a histogram method. If the cells are very small, then some cells may not contain any particle, or worse they could contain negative mass particles, thus the concentration would be negative in those cells. That is why, the size of the concentration cells should be coarser if adaptive or negative mass particles exist. Even without negative masses, the size of the concentration cells should be selected in consideration of the number of particles and domain size (or some diffusion length scale). Convergence behavior has been studied mathematically for instance by Raviart [28].

There are other types of methods to obtain a spatial distribution of concentration $C(x, t)$ from particle positions (e.g. the Mobile Window method, the Convolution Filter method). In this study we have used the first post-processing method (Fixed Windows).

4. Results and discussion

In this section, the new RWPT algorithm will be tested with the analytical solution Eq. (2.9). Then, it will be compared with the generalized analytical solution, for a diffusion problem with two interfaces and three different discontinuous diffusion coefficients and porosities, as described in subsection 3.3.1.

4.1. Time evolution of concentration profiles

Fig. 4.1 and Fig. 4.2 display the analytical vs. simulation results, at three times, of diffusion with one interface and two interfaces (where $D(x)$ and $\theta(x)$ are discontinuous). Fig. 4.1 has diffusion contrast $D_2/D_1 = 100$ and porosity contrast $\theta_2/\theta_1 = 4$ with the discontinuity located at $x = 0$. The values of diffusion and porosity for Fig. 4.2 are shown in Table 1. The initial source is at $x = -1$; it is located in the left subdomain with the lowest diffusion and porosity coefficients. Thus, in both figures, particles initially encounter an interface with negative reflection coefficient R . Particles are either reflected at the interfaces and stay in the subdomain, or they cross the interface and enter the next subdomain. The simulation results were obtained by using 100 million particles and setting the time step equal to final simulation time ($\Delta t = T_{SIMU}$). The fit is excellent in all cases, including near discontinuities.

Note in all tables, the coefficient D is dimensionless, as well as space and time units.

In Fig. 4.3, the histogram is the result obtained by the RWPT with ten million particles initially. The diffusion and porosity contrasts are given in Table 2. This result was obtained by setting the time step equal to the final simulation time,

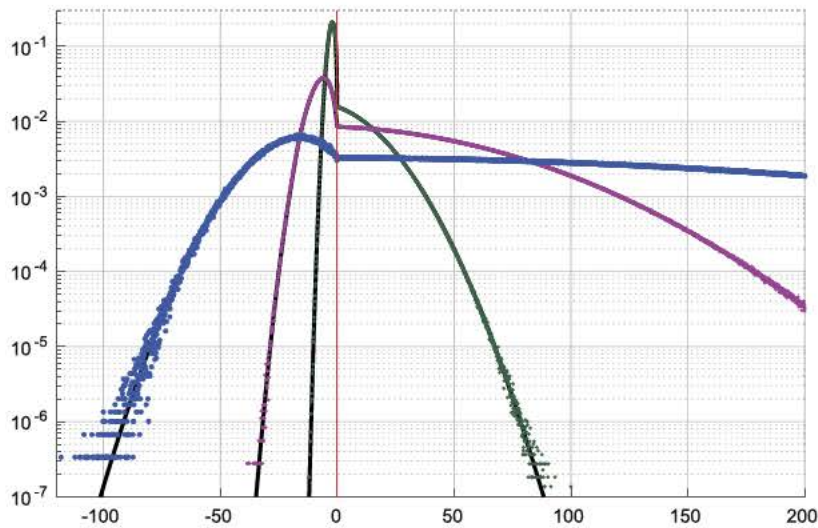


Fig. 4.1. Time evolution of concentration profiles using the negative mass algorithm. The vertical red line corresponds to the position of the interface $x = 0$. The green, magenta and blue bold dots correspond to the simulation results at three different times. The bold black curves correspond to the analytical solution of Eq. (2.9). (For interpretation of the colors in the figure(s), the reader is referred to the web version of this article.)

Table 1
Diffusion and porosity values of Fig. 4.2.

x	$]-\infty; 0]$	$[0; 100]$	$[100; +\infty[$
D	1	10^2	10^1
θ	0.25	1.00	0.50

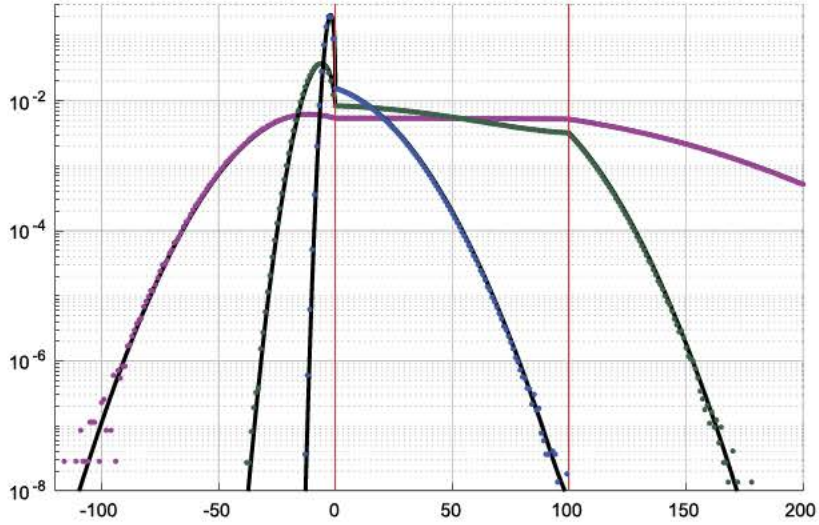


Fig. 4.2. Time evolution of concentration profiles using the Stop&Go algorithm with negative mass particles for 100 million particles. The red vertical lines correspond to the interfaces $x = 0$ and $x = 100$. The green, magenta and blue bold dots correspond to the simulation results at three different times. The bold black curves correspond to the semi-analytical solution of subsection 3.3.1.

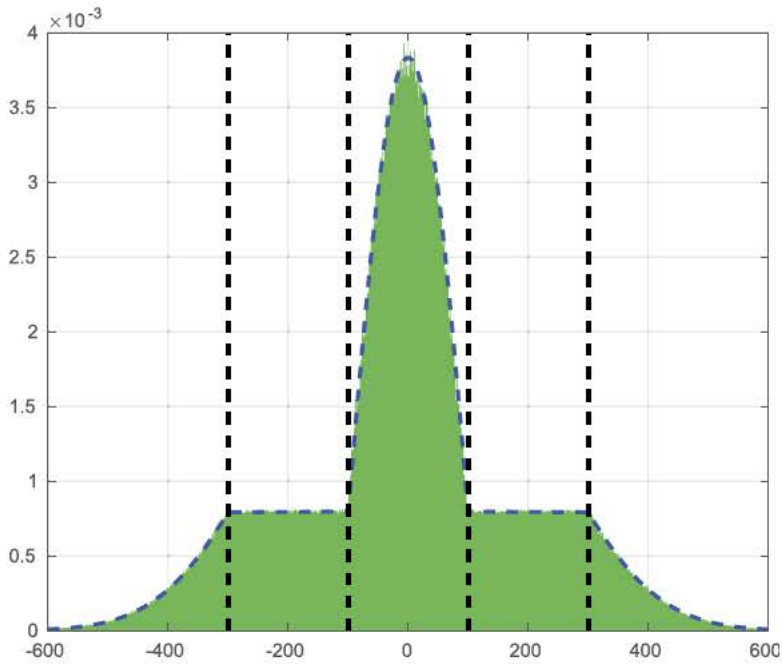


Fig. 4.3. Comparison between analytical (PDE) and numerical (RWPT) concentration histogram (in green) using negative mass particles, for a 1D infinite domain with an initial Dirac mass at $x_0 = 0$ ("source"). The diffusion and the porosity coefficients $D(x)$ and $\theta(x)$ are discontinuous at the black dashed lines (see Table 2). The dashed blue curve is the semi-analytical solution of the diffusion (see Algorithm 1).

Table 2
Diffusion and porosity contrasts of Fig. 4.3.

x	$]-\infty; -300]$	$[-300; -100]$	$[-100; 100]$	$[100; 300]$	$[300; +\infty[$
D	1	10^5	1	10^5	1
θ	10^{-1}	1	10^{-1}	1	10^{-1}

for more efficiency. Such fluctuations are inherent to the RWPT method for a finite number of particles, but they appear quite moderate here given the large contrast ratio of the discontinuous coefficients ($10/1$ for porosity, and $100,000/1$ for diffusion).

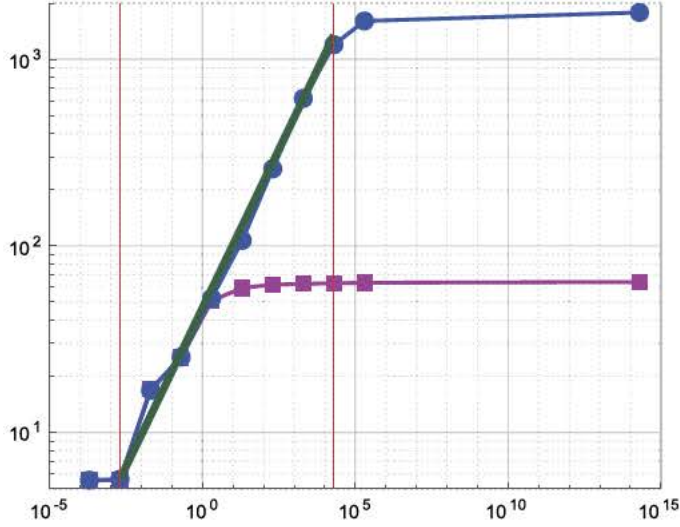


Fig. 4.4. CPU Time versus Final Simulation Time for 100 million particles. The bold magenta curve with squares corresponds to Fig. 4.1. The bold blue curve with circles corresponds to Fig. 4.2. The bold green line is a power law fit (exponent 0.34).

4.2. Discussion of CPU Time

Explicit time-stepping methods usually have a linear evolution of CPU Time vs. simulation time. We observe from Fig. 4.4 that the CPU Time of the Stop&Go algorithm behaves as a power law, then reaches a constant plateau in a second stage. In Fig. 4.4, the magenta curve with squares corresponds to the two-layer problem of Fig. 4.1, while the blue curve with circles corresponds to the three-layer problem of Fig. 4.2. For very small simulation time, particles have not yet reached the interface. Therefore, the algorithm does not need to deal with discontinuity, and the CPU Time remains constant. For intermediate simulation time, CPU Time evolves as the power 0.34 of simulation time T_{SIMU} (Fig. 4.4). This exponent depends probably on diffusion and porosity contrasts, number of interfaces, etc. Finally, as can be seen in Fig. 4.4, CPU Time reaches a plateau for $T_{SIMU} > 2$ for the two-layer problem, and for $T_{SIMU} > 2 \cdot 10^4$ for the three-layer problem.

For larger simulation times, more and more particles succeed in crossing the outer interfaces (after many trials). This is because the transmission probability $(1 - R)$, although small, is strictly non null. Once this crossing has occurred, particles only need to do a single step to reach their final position at time T_{SIMU} in the left or right semi-infinite layers. In summary, the computational performance of the negative mass Stop&Go RWPT scheme is encouraging; the CPU time evolves sub-linearly with simulation time, while it evolved linearly in previous RWPT methods.

4.3. Efficiency comparison with the previous method

In this subsection, Bechtold's method [17] is compared to the negative particles method proposed in this paper. The comparison is done on a test case of the diffusion of an initial source located at $x_0 = -1$ at time $t_1 = 1$ in a domain with one discontinuity located at $x = 0$. The porosity is constant throughout the domain, while the diffusion coefficient has a value $D_1 = 1$ on the left and $D_2 = 30$ on the right of the discontinuity. Fig. 4.5 plots the CPU Time and the normalized error versus number of particles. The normalized error $\bar{\epsilon}$ is calculated on a subdomain $[x_0 - \sqrt{2D_1t_1}; x_0 + \sqrt{2D_2t_1}]$ discretized in $N_{elements}$:

$$\bar{\epsilon} = \sqrt{\frac{1}{N_{elements}} \sum_{i=1}^{N_{elements}} \left(\frac{C_{Simu}(x_i; t_1)}{C_{Anal}(x_i; t_1)} - 1 \right)^2} \quad (4.1)$$

Fig. 4.5 shows that for Bechtold's method, the normalized error decreases with smaller time step sizes, however, the CPU Time increases. On the other hand, the Normalized Error of the negative particles method proposed in this paper decreases with the number of particles initially used, and in all cases, it is smaller than the ones of Bechtold's method, even for a small time step ($\Delta t = 10^{-3}$) (Notice, here, that with Bechtold's method from $N_{particles} = 10^6$ the error does not decrease anymore with the number of particles, because the error is intrinsic to the time step size). In addition, the CPU Time of the negative particles method is smaller than the one of Bechtold's method. In conclusion, the negative particle scheme performs better both in terms of accuracy and in terms of CPU Time efficiency.

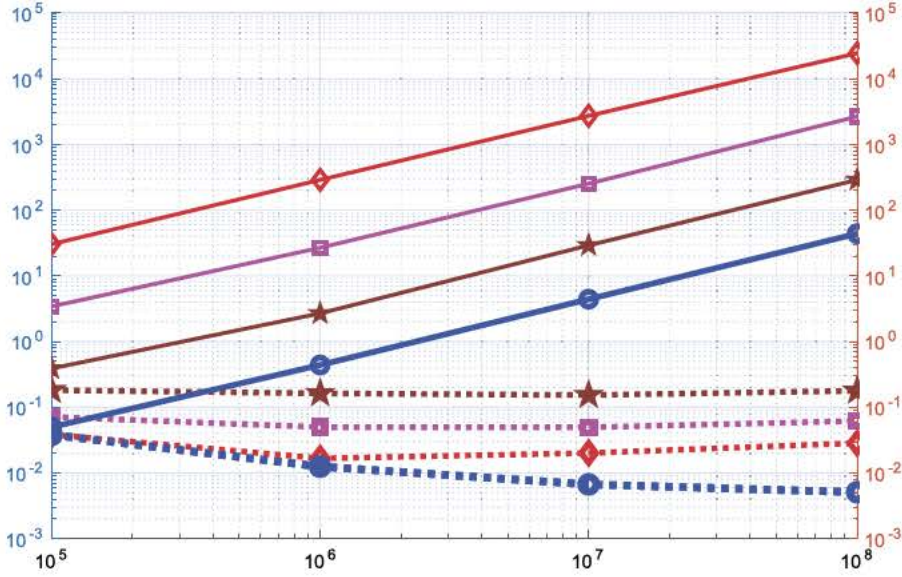


Fig. 4.5. CPU Time and Error versus initial Number of particles. The bold curves are the CPU Times. The dotted curves are the corresponding Errors. The blue color with circles corresponds to the negative particles method. The brown, magenta and red colors correspond to Bechtold's method with respectively a time step $\Delta t = 10^{-1}$, $\Delta t = 10^{-2}$ and $\Delta t = 10^{-3}$.

5. Conclusion and outlook

We have developed a new Stop&Go random walk algorithm with negative unit mass particles for discontinuous diffusion problems. It is based on comparisons of partial reflection/transmission schemes with analytical solutions for diffusion with discontinuous $D(x)$ and $\theta(x)$. This scheme keeps particles independent, although the appearance of negative masses may require special post-processing (the algorithm keeps the absolute mass value constant but leads to a growing number of particles). While this novel scheme may seem to add computational constraints, the gains from lifting restrictions on the time step outweigh these constraints.

The algorithm has been extended to multiple interfaces as well. Their validation and computational performance has been demonstrated. The scheme seems promising and is being currently extended to take into account a particle's velocity component (e.g. one diffusive sub-step followed by one advective sub-step) which is discontinuous if porosity is discontinuous, and in more complex 3D geometries (ongoing work).

Appendix A. Analytical solution for diffusion in a 3-layer medium

This appendix presents the detailed analytical solutions for diffusion in an infinite medium with 2 "interfaces" of discontinuity of the diffusion coefficient $D(x)$ and porosity $\theta(x)$, defining 3 layers with coefficients $(D_1; \theta_1)$, $(D_2; \theta_2)$, $(D_3; \theta_3)$. The interfaces are located at $x = x_{1:2}$ and $x = x_{2:3}$. This problem is described by the following equation system:

$$\begin{cases} \forall t > 0; \forall x \leq x_{1:2}; & \frac{\partial C_1}{\partial t}(x, t) = D_1 \frac{\partial^2 C_1}{\partial x^2}(x, t) \\ \forall t > 0; \forall x_{1:2} \leq x \leq x_{2:3}; & \frac{\partial C_2}{\partial t}(x, t) = D_2 \frac{\partial^2 C_2}{\partial x^2}(x, t) \\ \forall t > 0; \forall x \geq x_{2:3}; & \frac{\partial C_3}{\partial t}(x, t) = D_3 \frac{\partial^2 C_3}{\partial x^2}(x, t) \end{cases} \quad (\text{A.1a})$$

$$\begin{cases} \forall t \geq 0; & \lim_{x \rightarrow -\infty} C_1(x, t) = 0 \\ \forall t \geq 0; & \lim_{x \rightarrow +\infty} C_3(x, t) = 0 \end{cases} \quad (\text{A.1b})$$

$$\begin{cases} \forall t \geq 0; & C_1(x_{1:2}, t) = C_2(x_{1:2}, t) \\ \forall t \geq 0; & C_3(x_{2:3}, t) = C_2(x_{2:3}, t) \\ \forall t \geq 0; & -\theta_1 D_1 \frac{\partial C_1}{\partial x}(x_{1:2}, t) = -\theta_2 D_2 \frac{\partial C_2}{\partial x}(x_{1:2}, t) \\ \forall t \geq 0; & -\theta_3 D_3 \frac{\partial C_3}{\partial x}(x_{2:3}, t) = -\theta_2 D_2 \frac{\partial C_2}{\partial x}(x_{2:3}, t) \end{cases} \quad (\text{A.1c})$$

The solution is described for two cases of "initial" point sources $C(x, 0) = M_0 \cdot \delta(x - x_0)$ located at $x_0 < x_{1:2} < x_{2:3}$ and $C(x, 0) = M_0 \cdot \delta(x - x_1)$ located at $x_{1:2} < x_1 < x_{2:3}$. In the first case, the source is in the left layer, but similar solutions are obtained for any source position. These solutions are used in the text in relation to the generalization of our Random Walk algorithm, and for comparison/validation of results (Section 4, Fig. 4.2).

For a source located at left ($x_0 < x_{1:2}$) the initial condition for the diffusion problem of Eq. (A.1) is:

$$\begin{cases} \forall x \leq x_{1:2}; & C_1(x, 0) = \frac{M_0}{\theta_1} \delta(x - x_0) \\ \forall x_{1:2} \leq x \leq x_{2:3}; & C_2(x, 0) = 0 \\ \forall x \geq x_{2:3}; & C_3(x, 0) = 0 \end{cases} \quad (\text{A.2})$$

The solution of the discontinuous diffusion problem (Eq. (A.1)) with initial condition (A.2) is:

$$\begin{aligned} \forall t \geq 0; \forall x \leq x_{1:2}; \quad & \frac{\theta_1}{M_0} C_1(x, t) = G(x_0, 2D_1 t, x) + R_{1:2} G(-x_0 + 2x_{1:2}, 2D_1 t, x) \\ & + \sum_{i=0}^{+\infty} (1 - R_{1:2}) R_{2:3} (R_{2:3} R_{2:1})^i (1 - R_{2:1}) \times G\left(-x_0 + 2x_{1:2} + 2(i+1) \frac{\sqrt{D_1}}{\sqrt{D_2}} (x_{2:3} - x_{1:2}), 2D_1 t, x\right) \end{aligned} \quad (\text{A.3a})$$

$$\begin{aligned} \forall t \geq 0; \forall x_{1:2} \leq x \leq x_{2:3}; \quad & \frac{\theta_2}{M_0} C_2(x, t) = \sum_{i=0}^{+\infty} (1 - R_{1:2}) (R_{2:3} R_{2:1})^i \\ & \times \left(G\left(\frac{\sqrt{D_2}}{\sqrt{D_1}} (x_0 - x_{1:2}) - (2i+1) (x_{2:3} - x_{1:2}) + x_{2:3}, 2D_2 t, x\right) + R_{2:3} \right. \\ & \left. \times G\left(-\frac{\sqrt{D_2}}{\sqrt{D_1}} (x_0 - x_{1:2}) + (2i+1) (x_{2:3} - x_{1:2}) + x_{2:3}, 2D_2 t, x\right) \right) \end{aligned} \quad (\text{A.3b})$$

$$\begin{aligned} \forall t \geq 0; \forall x \geq x_{2:3}; \quad & \frac{\theta_3}{M_0} C_3(x, t) = \sum_{i=0}^{+\infty} (1 - R_{1:2}) (R_{2:3} R_{2:1})^i (1 - R_{2:3}) \\ & \times G\left(\frac{\sqrt{D_3}}{\sqrt{D_1}} (x_0 - x_{1:2}) + (2i+1) \frac{\sqrt{D_3}}{\sqrt{D_2}} (x_{1:2} - x_{2:3}) + x_{2:3}, 2D_3 t, x\right) \end{aligned} \quad (\text{A.3c})$$

And the solution of Eq. (A.1) with the initial condition

$$\begin{cases} \forall x \leq x_{1:2}; & C_1(x, 0) = 0 \\ \forall x_{1:2} \leq x \leq x_{2:3}; & C_2(x, 0) = \frac{M_0}{\theta_1} \delta(x - x_1) \\ \forall x \geq x_{2:3}; & C_3(x, 0) = 0 \end{cases} \quad (\text{A.4})$$

is:

$$\begin{aligned} \forall t \geq 0; \forall x \leq x_{1:2}; \quad & \frac{\theta_1}{M_0} C_1(x, t) = (1 - R_{2:1}) \sum_{i=0}^{+\infty} (R_{2:3} R_{2:1})^i \\ & \times \left(G\left(x_{1:2} + \sqrt{\frac{D_1}{D_2}} (2i (x_{2:3} - x_{2:1}) + x_0 - x_{1:2}), 2D_1 t, x\right) \right. \\ & \left. + R_{2:3} G\left(x_{1:2} + \sqrt{\frac{D_1}{D_2}} (2i (x_{2:3} - x_{2:1}) + 2x_{2:3} - x_0 - x_{1:2}), 2D_1 t, x\right) \right) \end{aligned} \quad (\text{A.5a})$$

$$\begin{aligned} \forall t \geq 0; \forall x_{1:2} \leq x \leq x_{2:3}; \quad & \frac{\theta_2}{M_0} C_2(x, t) = -G(x_0, 2D_2 t, x) + \sum_{i=0}^{+\infty} (R_{2:3} R_{2:1})^i \\ & \times (G(2i (x_{2:3} - x_{1:2}) + x_0, 2D_2 t, x) + G(2i (x_{1:2} - x_{2:3}) + x_0, 2D_2 t, x) \\ & + R_{2:3} G(2i (x_{2:3} - x_{1:2}) + 2x_{2:3} - x_0 - x_{1:2}, 2D_2 t, x) \\ & + R_{2:1} G(2i (x_{1:2} - x_{2:3}) + 2x_{1:2} - x_0 - x_{2:3}, 2D_2 t, x)) \end{aligned} \quad (\text{A.5b})$$

$$\begin{aligned}
\forall t \geq 0; \forall x \geq x_{2:3}; \quad & \frac{\theta_3}{M_0} C_3(x, t) = (1 - R_{2:3}) \sum_{i=0}^{+\infty} (R_{2:1} R_{2:3})^i \\
& \times \left(G \left(x_{2:3} + \sqrt{\frac{D_3}{D_2}} (2i(x_{1:2} - x_{2:3}) + x_0 - x_{2:3}), 2D_3 t, x \right) \right. \\
& \left. + R_{2:1} G \left(x_{2:3} + \sqrt{\frac{D_3}{D_2}} (2i(x_{1:2} - x_{2:3}) + 2x_{1:2} - x_0 - x_{2:3}), 2D_3 t, x \right) \right)
\end{aligned} \tag{A.5c}$$

The above solutions have been checked by direct substitution in Eq. (A.1a) and the initial and boundary conditions Eq. (A.1b), Eq. (A.1c) and Eq. (A.2).

The infinite series obtained in this section for concentration $C(x, t)$ have the form of a function $h(x, t)$ defined as:

$$h(x, t) = \sum_{n=0}^{+\infty} \frac{A}{\sqrt{t}} z^n \exp\left(-\frac{(x + Cn + D)^2}{Bt}\right) \tag{A.6}$$

with $B, t > 0$; $x, A, C, D \in \mathbb{R}$ and $z = R_{2:1} R_{2:3}$ (product of partial reflection coefficients). Their convergence is studied in the next appendix (Appendix B).

Appendix B. Study of the convergence and continuity of the series h

In this appendix, we study the convergence of the infinite series $h(x, t)$ (A.6) which has the form of the solution found in Appendix A. This solution (concentration $C(x, t)$) was used in Fig. 4.2 to validate the Random Walk Particle Tracking model proposed in this paper for discontinuous diffusion.

B.1. Pointwise convergence using d'Alembert criteria

Theorem 1 (d'Alembert Ratio test [29]). Let $(a_n, n \in \mathbb{N})$ be a sequence of complex numbers such that $L = \lim_{n \rightarrow +\infty} \frac{|a_{n+1}|}{|a_n|}$ exists.

If $L < 1$, then the series $\sum_{n=0}^{+\infty} a_n$ converges absolutely. Thus, $\sum_{n=0}^{+\infty} a_n$ is pointwise convergent.

If $L > 1$, then the series $\sum_{n=0}^{+\infty} a_n$ is divergent.

If $L = 1$, then the case is undecided.

Using Theorem 1, we now show that our series $h(x, t)$ is pointwise convergent. This series is of the form $h(x, t) = \sum_{n=0}^{+\infty} U_n(x, t)$, where:

$$U_n = \frac{A}{\sqrt{t}} z^n \exp\left(-\frac{(x + Cn + D)^2}{Bt}\right) \tag{B.1}$$

$$\frac{|U_{n+1}|}{|U_n|} = |z| \exp\left(-\frac{(x + C(n+1) + D)^2 - (x + Cn + D)^2}{Bt}\right) \tag{B.2}$$

$$\frac{|U_{n+1}|}{|U_n|} = |z| \exp\left(-\frac{2xC + C^2 + 2DC}{Bt}\right) \exp\left(\frac{-2C^2 n}{Bt}\right) \tag{B.3}$$

If $C = 0$, then the series converges for $|z| < 1$ and $B, t > 0$; $x, A, D \in \mathbb{R}$, $h(t, x) = \frac{A}{\sqrt{t}} \frac{1}{1-z} \exp\left(-\frac{(x+D)^2}{Bt}\right)$. This case occurs if the distance between two interfaces $(|x_{1:2} - x_{2:3}|)$ goes to zero (we may dismiss this case here).

Otherwise, if $C \neq 0$, then $\frac{|U_{n+1}|}{|U_n|} \rightarrow_{n \rightarrow +\infty} 0$. By the d'Alembert Ratio test, the series h converges $\forall z \in \mathbb{C}$; $\forall B > 0, \forall t > 0$; $\forall x, A, C, D \in \mathbb{R}$.

In conclusion, the series $h(x, t)$ and the analytical concentrations solutions (Eqs. (3.8) and (3.9)) converge pointwise in all cases of interest.

B.2. Uniform convergence

Theorem 2 ([29]). Assume (f_n) is a sequence of functions defined on E , and assume $|f_n(x)| \leq M_n$ ($x \in E, n = 1, 2, 3, \dots$). Then $\sum f_n$ converges uniformly on E if $\sum M_n$ converges.

The infinite series $h(x, t)$ is of the form:

$$h(x, t) = \sum_{n=0}^{+\infty} A z^n \exp\left(-\frac{Bt \ln(t) + 2(x + Cn + D)^2}{2Bt}\right) \tag{B.4}$$

Let us define $g_n(x, t)$ as:

$$g_n(x, t) = -\frac{Bt \ln(t) + 2(x + Cn + D)^2}{2Bt} \quad (\text{B.5})$$

For $t \geq 1$ we have $g_n \leq 0$. Thus,

$$\left| Az^n \exp\left(-\frac{Bt \ln(t) + 2(x + Cn + D)^2}{2Bt}\right) \right| \leq |A| |z|^n \quad (\text{B.6})$$

Since the series $\sum_{n=0}^{+\infty} |A| |z|^n$ converges for $|z| < 1$, h is uniformly convergent on $\mathbb{R} \times [1; +\infty[$.

For $0 < t \leq 1$ we have $\frac{-B}{e} \leq Bt \ln(t) \leq 0$.

- First, if $C > 0$ and for a fixed $x_0 \in \mathbb{R}$; $\exists n_1 / \forall n \geq n_1; \forall x \geq x_0; Bt \ln(t) + 2(x + Cn + D)^2 \geq Bt \ln(t) + 2(x_0 + Cn + D)^2 \geq 0$. Hence, the series h converges uniformly on $[x_0; +\infty[\times]0; 1]$.
- Secondly, if $C < 0$ and for a fixed $x_0 \in \mathbb{R}$; $\exists n_2 / \forall n \geq n_2; \forall x \leq x_0; Bt \ln(t) + 2(-x - Cn - D)^2 \geq Bt \ln(t) + 2(-x_0 - Cn - D)^2 \geq 0$. The series h converges uniformly on $]0; 1] \times]-\infty; x_0]$.

Theorem 3 ([29]). *If (f_n) is a sequence of continuous functions on E , and if $f_n \rightarrow f$ uniformly on E , then f is continuous on E .*

Consequence For $z \in \mathbb{C}$ such that $|z| < 1$, h is continuous with respect to (x, t) on $\mathbb{R} \times]0; +\infty[$.

Conclusion In all cases of interest, the analytical infinite series concentration solutions (Eqs. (3.8) and (3.9)) are pointwise convergent and continuous with respect to (x, t) on $\mathbb{R} \times]0; +\infty[$.

References

- [1] M. Sahimi, Fractal and superdiffusive transport and hydrodynamic dispersion in heterogeneous porous media, *Transp. Porous Media* 13 (1) (1993) 3–40, <https://doi.org/10.1007/BF00613269>.
- [2] M. Spiller, R. Ababou, J. Koengeter, Alternative approach to simulate transport based on the master equation, in: *Tracers and Modelling in Hydrogeology, Proceedings of the TraM'2000 Conference held at Liège, Belgium, May 2000*, in: IAHS Publ., vol. 262, 2000.
- [3] P.K. Kang, T. Le Borgne, M. Dentz, O. Bour, R. Juanes, Impact of velocity correlation and distribution on transport in fractured media: field evidence and theoretical model, *Water Resour. Res.* 51 (2015) 940–959, <https://doi.org/10.1002/2014WR015799>.
- [4] F. Delay, J. Bodin, Time domain random walk method to simulate transport by advection-dispersion and matrix diffusion in fracture networks, *Geophys. Res. Lett.* 28 (21) (2001) 4051–4054.
- [5] J. Bodin, From analytical solutions of solute transport equations to multidimensional time-domain random walk (TDRW) algorithms, *Water Resour. Res.* 51 (2015) 1860–1871, <https://doi.org/10.1002/2014WR015910>.
- [6] B. Noetinger, D. Roubinet, J. De Dreuzy, A. Russian, P. Gouze, T. Le Borgne, M. Dentz, F. Delay, Random walk methods for modeling hydrodynamic transport in porous and fractured media from pore to reservoir scale, *Transp. Porous Media* 115 (2) (2016) 345–385, <https://doi.org/10.1007/s1142-016-0693-z>, hal-014449131.
- [7] E.M. LaBolle, G.E. Fogg, A.F.B. Tompson, Random-walk simulation of transport in heterogeneous porous media: local mass-conservation problem and implementation methods, *Water Resour. Res.* 32 (3) (1996) 583–593, <https://doi.org/10.1029/95WR03528>.
- [8] M. Spiller, R. Ababou, T. Becker, A. Fadili, J. Koengeter, Mass Transport with Heterogeneous Diffusion: Interpolation Schemes for Random Walks, in: *8th Annual Conference of the International Association for Mathematical Geology, IAMG 2002, Berlin, Germany, 15–20 September 2002*, Selbstverlag der Alfred-Wegener-Stiftung, Berlin, 2002, pp. 305–310 (Terra Nostra: Schriften der Alfred-Wegener-Stiftung, 4, 2).
- [9] G.J.M. Uffink, A random-walk method for the simulation of macrodispersion in a stratified aquifer, in: *Relation of Groundwater Quality and Quantity*, in: IAHS Publ., vol. 146, Int. Assoc. of Hydrol. Sci., Gentbrugge, Belgium, 1985, pp. 103–114.
- [10] A.C. Bagtzoglou, A.F.B. Tompson, D.E. Dougherty, Projection functions for particle grid methods, *Numer. Methods Partial Differ. Equ.* 8 (1992) 325–340.
- [11] E.M. LaBolle, J. Quastel, G.E. Fogg, Diffusion theory for transport in porous media: transition-probability densities of diffusion processes corresponding to advection-dispersion equations, *Water Resour. Res.* 34 (7) (1998) 1685–1693, <https://doi.org/10.1029/98WR00319>.
- [12] P. Ackerer, Propagation d'un fluide en aquifère poreux saturé en eau. Prise en compte et localisation des hétérogénéités par outils théoriques et expérimentaux, Ph.D. thesis, Univ. Louis Pasteur de Strasbourg, Strasbourg, France, 1985.
- [13] C. Cordes, H. Daniels, G. Rouvé, A new very efficient algorithm for particle tracking in layered aquifers, in: D.B. Sari, et al. (Eds.), *Computer Methods in Water Resources II, Groundwater Modelling and Pressure Flow*, vol. 1, Springer, Germany, 1991, pp. 41–55.
- [14] K. Semra, P. Ackerer, R. Mose, Three dimensional groundwater quality modeling in heterogeneous media, in: L.C. Wrobel, C.A. Brebbia (Eds.), *Water Pollution II: Modelling, Measuring and Prediction*, Southampton, UK, 1993, pp. 3–11.
- [15] H. Hoteit, R. Mose, A. Younes, F. Lehmann, P. Ackerer, Three-dimensional modeling of mass transfer in porous media using the mixed hybrid finite elements and the random-walk methods, *Math. Geol.* 34 (4) (2002) 435–456, <https://doi.org/10.1023/A:1015083111971>.
- [16] D.H. Lim, Numerical study of nuclide migration in a nonuniform horizontal flow field of a high-level radioactive waste repository with multiple canisters, *Nucl. Technol.* 156 (2) (2006) 222–245.
- [17] M. Bechtold, J. Vanderborght, O. Ippisch, H. Vereecken, Efficient random walk particle tracking algorithm for advective-dispersive transport in media with discontinuous dispersion coefficients and water contents, *Water Resour. Res.* 47 (2011) W10526, <https://doi.org/10.1029/2010WR010267>.
- [18] A. Lejay, G. Pichot, Simulating diffusion processes in discontinuous media: a numerical scheme with constant time steps, *J. Comput. Phys.* 231 (2012) 7299–7314, <https://doi.org/10.1016/j.jcp.2012.07.011>.
- [19] A. Lejay, G. Pichot, Simulating diffusion processes in discontinuous media: benchmark tests, *J. Comput. Phys.* 2016 (314) (2016) 384–413, <https://doi.org/10.1016/j.jcp.2016.03.003>.
- [20] P. Ackerer, R. Mose, Comment on "Diffusion theory for transport in porous media: Transition-probability densities of diffusion processes corresponding to advection-dispersion equations" by Eric M. LaBolle et al., *Water Resour. Res.* 36 (3) (2000) 819–821, <https://doi.org/10.1029/1999WR900326>.
- [21] L. Schwartz, *Théorie des distributions*, 2 volumes, Hermann, 1950/1951, nouvelle édition, 1966.

- [22] H. Risken, *The Fokker-Planck Equation*, Springer, Heidelberg, New York, 1996.
- [23] M. Dentz, P. Gouze, A. Russian, J. Dweik, F. Delay, Diffusion and trapping in heterogeneous media: an inhomogeneous continuous time random walk approach, *Adv. Water Resour.* (ISSN 0309-1708) 49 (2012) 13–22, <https://doi.org/10.1016/j.advwatres.2012.07.015>.
- [24] D.T. Gillespie, E. Seitaridou, *Simple Brownian Diffusion*, Oxford University Press, 2013.
- [25] A.F.B. Tompson, L.W. Gelhar, Numerical-simulation of solute transport in 3-dimensional, randomly heterogeneous porous-media, *Water Resour. Res.* 26 (10) (1990) 2541–2562, <https://doi.org/10.1029/WR026i010p02541>.
- [26] H.S. Carslaw, J.C. Jaeger, *Conduction of Heat in Solids*, Clarendon, Oxford, 1959, pp. 363–365.
- [27] F. Delay, P. Ackerer, C. Danquigny, Simulating solute transport in porous or fractured formations using random walk particle tracking a review, *Vadose Zone J.* 4 (2005), <https://doi.org/10.2136/vzj2004.0125>.
- [28] P.A. Raviart, Particle approximation of linear hyperbolic equation of the first order, in: *Numerical Methods in Fluids Dynamics*, in: *Lectures Notes in Math.*, Springer Verlag, 1983 (Chap. 1).
- [29] W. Rudin, *Principles of Mathematical Analysis*, McGraw-Hill Book Company, New York, 1976.